

# Hydrothermally Stable $\text{WO}_3/\text{ZrO}_2\text{-Ce}_{0.6}\text{Zr}_{0.4}\text{O}_2$ Catalyst for the Selective Catalytic Reduction of $\text{NO}$ with $\text{NH}_3$

Tinku Baidya · Andreas Bernhard ·  
Martin Elsener · Oliver Kröcher

Published online: 22 February 2013  
© Springer Science+Business Media New York 2013

**Abstract** A new catalyst  $\text{WO}_3/\text{ZrO}_2\text{-Ce}_{0.6}\text{Zr}_{0.4}\text{O}_2$  (15 wt %  $\text{WO}_3/\text{ZrO}_2\text{:Ce}_{0.6}\text{Zr}_{0.4}\text{O}_2 = 50:50$ ) has been developed for the selective catalytic reduction of  $\text{NO}$  with  $\text{NH}_3$ . The redox component  $\text{Ce}_{0.6}\text{Zr}_{0.4}\text{O}_2$  was dispersed on the surface of acidic  $\text{WO}_3/\text{ZrO}_2$  by the solution combustion method showing the best  $\text{NO}_x$  reduction efficiency among the catalysts prepared by various modes of mixing of the components. The catalyst has been characterized by XRD, Raman spectroscopy and  $\text{NH}_3$ -TPD. A  $\text{NO}_x$  reduction efficiency of more than 90 % was obtained between 300 and 500 °C at  $\alpha = \text{NH}_{3,\text{in}}/\text{NO}_{x,\text{in}} = 1$ . The catalyst showed stable  $\text{NO}_x$  reduction efficiency after hydrothermal ageing at 700 °C. Sulfur poisoning promoted the  $\text{NO}_x$  reduction efficiency at high temperatures at the expense of a reduced activity at lower temperatures, but the catalyst could be fully regenerated by heating in  $\text{O}_2$  at 650 °C.

**Keywords** Selective catalytic reduction · SCR · Catalyst · Rare earth metal oxides

## 1 Introduction

$\text{NO}_x$  abatement from diesel engine exhaust is one of the major challenges in environmental catalysis.  $\text{NO}_x$  gases are the major source of pollution and photochemical smog formation. The most efficient technology to remove  $\text{NO}_x$  from stationary sources is the selective catalytic reduction (SCR) of  $\text{NO}_x$  by ammonia ( $4\text{NH}_3 + 4\text{NO} + \text{O}_2 \rightarrow 4\text{N}_2 + 6\text{H}_2\text{O}$ ) [1–4]. Reduction of  $\text{NO}_x$  from diesel engine emissions

requires a highly efficient catalyst operating over a temperature range of 200–500 °C at high space velocity. Under certain circumstances such as diesel particulate filter (DPF) regeneration, the diesel exhaust gas temperature can even go up to slightly above 700 °C [5]. For light-duty vehicles its use is restricted by the complexity and large dimensions of the SCR system that must incorporate also a tank for the aqueous urea solution ( $\text{NH}_3$  precursor), a urea hydrolysis catalyst and eventually an  $\text{NH}_3$  slip catalyst [6]. Other critical aspects are the limited hydrothermal stability and the potentially toxic emissions of currently available SCR catalysts [7–9].

Among metal oxide-based SCR catalysts, commercially used  $\text{V}_2\text{O}_5/\text{WO}_3\text{-TiO}_2$  catalysts are highly active, but serious concern exists with respect to high temperature stability and sensitivity to phosphorus [2]. Manganese based catalysts also works very well at low temperature, but  $\text{NO}$  conversion is decreased significantly above 350 °C [10–18] and they easily deactivate by sulfur.

Recently, ceria-based SCR catalysts have attracted much attention due to their advantageous redox properties [14–23] and ceria-promoted acidic zirconia systems seem to be particularly attractive [24]. For instance, by using  $\text{Ce}_{1-x}\text{Zr}_x\text{O}_2$  as redox component  $\text{NO}_x$  reduction efficiency is maximized [19] and hydrothermal stability may be further enhanced by dispersing on a stable high surface acidic oxide. The activity is further enhanced by the addition of acidic components to bind ammonia, such as vanadate, tungstate or niobate [19, 22, 25]. However, the acidic component dispersed on the metal oxide surface tends to separate out under hydrothermal ageing at high temperatures initiated by sintering of the surface. Tungstate ( $\text{WO}_3$ ) is not only useful as acidic component but can also function as stabilizer for the underlying metal oxide. It has been found, for example, that a layer of  $\text{WO}_3$  stabilizes anatase

T. Baidya · A. Bernhard · M. Elsener · O. Kröcher (✉)  
Paul Scherrer Institut, OVGA/112, 5232 Villigen PSI,  
Switzerland  
e-mail: oliver.kroecher@psi.ch

TiO<sub>2</sub> and vice versa at temperatures up to 800 °C. Similarly, WO<sub>3</sub> dispersed on ZrO<sub>2</sub> may keep the tungstate species stable and, consequently, preserve the amount of acidic sites at the surface. If WO<sub>3</sub>/ZrO<sub>2</sub> and CeO<sub>2</sub>-ZrO<sub>2</sub> are combined, Ce<sub>1-x</sub>Zr<sub>x</sub>O<sub>2</sub> may disperse on the high surface WO<sub>3</sub>/ZrO<sub>2</sub> thereby maximizing the NO<sub>x</sub> reduction efficiency and preventing the loss of redox activity of Ce<sub>1-x</sub>Zr<sub>x</sub>O<sub>2</sub> due to sintering of the surface at high temperatures.

In this paper, we report a new mixed phase oxide catalyst, 15 wt % WO<sub>3</sub>/ZrO<sub>2</sub>-Ce<sub>1-x</sub>Zr<sub>x</sub>O<sub>2</sub> that shows high NO<sub>x</sub> reduction efficiency with NH<sub>3</sub>. The catalyst was characterized by XRD and NH<sub>3</sub>-TPD techniques. The catalyst performance was tested under various conditions including tests with urea solution, representative for SCR systems aboard of diesel vehicles.

## 2 Experimental

### 2.1 Catalysts Preparation and Characterization

The catalysts were prepared following different methods including the solution combustion method [26] and incipient wetness impregnation. 15 wt % WO<sub>3</sub>/ZrO<sub>2</sub>-Ce<sub>0.6</sub>Zr<sub>0.4</sub>O<sub>2</sub> was made in two steps as following.

In the first step, 15 wt % WO<sub>3</sub>/ZrO<sub>2</sub> was prepared by dissolving ammonium tungstate in a NH<sub>3</sub> solution and adding ZrO<sub>2</sub>. The suspension was evaporated to dryness. The solid was dried in air at 120 °C for 6 h and then calcined at 650 °C for 5 h.

In the second step, 15 wt % WO<sub>3</sub>/ZrO<sub>2</sub> was mixed with the other component Ce<sub>0.6</sub>Zr<sub>0.4</sub>O<sub>2</sub> by two different methods. This was done a) by forming Ce<sub>0.6</sub>Zr<sub>0.4</sub>O<sub>2</sub> phase directly in presence of WO<sub>3</sub>/ZrO<sub>2</sub> suspended in a Ce and Zr precursor solution, or b) by ball milling of a mixture of 15 wt % WO<sub>3</sub>/ZrO<sub>2</sub> and Ce<sub>0.6</sub>Zr<sub>0.4</sub>O<sub>2</sub> phases in a 50:50 ratio.

The first method a) of preparation could be accomplished by solution combustion method as well as co-precipitation method, commonly called CP catalysts. In the solution combustion method, an aqueous solution of (NH<sub>4</sub>)<sub>2</sub>Ce(NO<sub>3</sub>)<sub>6</sub>, ZrO(NO<sub>3</sub>)<sub>2</sub> and C<sub>2</sub>H<sub>5</sub>NO<sub>2</sub> (fuel) was prepared in the molar ratio 0.6:0.4:0.51. 15 wt % WO<sub>3</sub>/ZrO<sub>2</sub> was added to the solution forming a suspension solution and kept at 400 °C in the furnace. After evaporation at the point of complete drying the mixture ignited and the combustion product was obtained in a minute. In this preparation method, ¼ of the stoichiometrically calculated amount of fuel was used to avoid formation of voluminous oxides. This sample was marked SCM. In the co-precipitation method, the hydroxides were precipitated from a solution of ZrO(NO<sub>3</sub>)<sub>2</sub> and (NH<sub>4</sub>)<sub>2</sub>Ce(NO<sub>3</sub>)<sub>6</sub> and stirred for 6 h for homogeneous mixing. Then, 15 wt % WO<sub>3</sub>/ZrO<sub>2</sub> was added to the hydroxides suspension and the

resulting mixture was stirred until complete evaporation. The precipitate was dried at 120 °C for 3 h and then calcined at 650 °C for 5 h. The samples obtained by using this method was marked 'Co-prep'.

In the second method b), the Ce<sub>0.6</sub>Zr<sub>0.4</sub>O<sub>2</sub>, used in the ball milling (BM) mixing, was also prepared by both solution combustion as well as co-precipitation method as described above and was marked by the same abbreviations SCM and Co-prep, respectively.

10 wt % WO<sub>3</sub>/Ce<sub>0.6</sub>Zr<sub>0.4</sub>O<sub>2</sub> was prepared by the wet impregnation method. Ammonium tungstate was dissolved in an ammonia solution and added to Ce<sub>0.6</sub>Zr<sub>0.4</sub>O<sub>2</sub> such that it just wets the oxides. The resulting product was dried in air at 120 °C for 3 h and calcined at 650 °C for 5 h. This sample was marked IMP.

The catalysts were coated on cordierite honeycombs following previous described methods [8]. The catalyst loading was ~200 mg/cc.

X-ray diffraction measurements were carried out on a Bruker D8 Advance diffractometer using Cu K<sub>α</sub> radiation. The XRD patterns were collected over the 2θ range of 20° to 70° at a step size of 0.01°. To minimize the influence of texture, the samples were rotated during each measurement.

Ammonia Temperature-Programmed Desorption (NH<sub>3</sub>-TPD) was applied to measure the surface acidity of the materials and check their NH<sub>3</sub> storage capacities (ASC, expressed in mL/g). For this purpose, 200 mg powder catalyst were placed in a quartz U-shaped down-flow reactor (total length: 150 mm; internal diameter: 8 mm). The temperature was measured with a thermocouple located inside the reactor. In a first step, the sample was pre-treated in a flow of 30 mL/min He at 500 °C for 30 min. Ammonia adsorption was carried out for 15 min at 50 °C using a flow of 30 mL/min of 5 vol. % NH<sub>3</sub>/He. After purging at 50 °C for 1 h with pure He, the desorption of NH<sub>3</sub> was monitored with a Thermal Conductivity Detector (TCD) during heating up to 650 °C with 10 K/min.

### 2.2 Catalytic Activity Tests

The NO SCR activity with NH<sub>3</sub> gas was tested between 200 and 550 °C by feeding 1000 ppm NO, 1000 ppm NH<sub>3</sub>, 10 % O<sub>2</sub>, 5 % H<sub>2</sub>O and N<sub>2</sub> into a quartz plug-flow reactor at a gas hourly space velocities (GHSV) of 50,000 h<sup>-1</sup>. The resulting NO, NO<sub>2</sub>, N<sub>2</sub>O and unreacted NH<sub>3</sub> were quantified with a Nicolet Magna-IR 560 FTIR spectrometer [8]. The NO<sub>x</sub> reduction efficiency (DeNO<sub>x</sub>) was calculated as follows:

$$\text{DeNO}_x(\%) = \frac{\text{NO}_{x,\text{in}} - \text{NO}_{x,\text{out}}}{\text{NO}_{x,\text{in}}} \times 100$$

where  $\text{NO}_x$  is the sum of  $\text{NO}$  and  $\text{NO}_2$  concentrations.

Besides the equimolar dosage of  $\text{NO}_x$  and  $\text{NH}_3$ , the  $\text{NH}_3$  concentration was gradually increased from 100 to 1500 ppm at a constant  $\text{NO}$  concentration of 1000 ppm for assessing the ammonia slip of the catalyst (surface acidity), its redox potential and its ammonia oxidation potential.

### 3 Results and Discussions

The catalyst contains 15 wt %  $\text{WO}_3/\text{ZrO}_2$  as acid and  $\text{Ce}_{1-x}\text{Zr}_x\text{O}_2$  as redox component. To find the best composition regarding  $x$ , the  $\text{NO}$  SCR activity over 15 wt %  $\text{WO}_3/\text{ZrO}_2\text{-Ce}_{1-x}\text{Zr}_x\text{O}_2$  was tested with  $x = 0.0\text{--}0.5$ . The reference material 10 wt %  $\text{WO}_3/\text{ZrO}_2\text{-CeO}_2$  showed high  $\text{NO}_x$  reduction efficiency at all temperatures. The  $\text{NO}_x$  reduction efficiency over the  $\text{WO}_3/\text{ZrO}_2\text{-Ce}_{1-x}\text{Zr}_x\text{O}_2$  catalysts did not change much with increasing Zr concentration from  $x = 0.0$  to  $0.5$ , except slightly lower  $\text{NO}_x$  conversion at high temperatures. At high temperatures, slightly more  $\text{NH}_3$  oxidation occurred for higher Zr contents up to  $x = 0.4$ . At  $x = 0.5$ , a lower activity was observed at lower temperatures. Therefore, since the optimum Zr content also enhances both the redox activity and the hydrothermal stability, we choose  $\text{Ce}_{0.6}\text{Zr}_{0.4}\text{O}_2$  ( $x = 0.4$ ) as composition for the redox component in the target catalyst.

The mode of mixing of the components in the catalyst may change the  $\text{NO}_x$  reduction efficiency. It can be done in two ways: as prepared  $\text{Ce}_{0.6}\text{Zr}_{0.4}\text{O}_2$  can be added to  $\text{WO}_3/\text{ZrO}_2$  and then mixed by ball milling (marked BM) or  $\text{Ce}_{0.6}\text{Zr}_{0.4}\text{O}_2$  can be crystallized directly from the precursors on the  $\text{WO}_3/\text{ZrO}_2$  surface (marked CP). Figure 1 shows a comparison of the  $\text{NO}_x$  reduction efficiency over these catalysts of the common formula 15 wt %  $\text{WO}_3/\text{ZrO}_2\text{-Ce}_{0.6}\text{Zr}_{0.4}\text{O}_2$ . Ball milling of  $\text{WO}_3/\text{ZrO}_2$  and  $\text{Ce}_{0.6}\text{Zr}_{0.4}\text{O}_2$  resulted in a much lower activity as compared to the later method. The  $\text{Ce}_{0.6}\text{Zr}_{0.4}\text{O}_2$  component in BM and CP catalysts could be prepared by both the solution combustion method and the co-precipitation method. Obviously, the CP catalysts were generally more active than the BM catalysts. In the BM catalysts, when  $\text{Ce}_{0.6}\text{Zr}_{0.4}\text{O}_2$  was prepared by the co-precipitation method (Co-prep), it showed a higher  $\text{NO}_x$  reduction efficiency than the same catalyst with  $\text{Ce}_{0.6}\text{Zr}_{0.4}\text{O}_2$  prepared by solution combustion (SCM). Although  $\text{WO}_3/\text{ZrO}_2$  was the common component used in all catalyst preparations, the close proximity of redox sites and acidic sites in the CP catalysts seems to be decisive to achieve high  $\text{NO}_x$  reduction efficiency. It seems to be reasonable to assume that  $\text{Ce}_{0.6}\text{Zr}_{0.4}\text{O}_2$  crystallites could form on the surface and were distributed more homogeneously in the CP catalysts.

Since the CP catalyst from solution combustion was the easiest to prepare, we continued with this type for the further studies. The potential formation of a  $\text{Ce}_{0.6}\text{Zr}_{0.4}\text{O}_2$  solid solution on the  $\text{WO}_3/\text{ZrO}_2$  surface in the 10 wt %  $\text{WO}_3/\text{ZrO}_2\text{-Ce}_{0.6}\text{Zr}_{0.4}\text{O}_2$  (SCM) catalyst was examined by XRD in Fig. 2. For the purpose of comparison of the peak positions in the mixed oxides, pure  $\text{Ce}_{0.6}\text{Zr}_{0.4}\text{O}_2$  phase and 10 wt %  $\text{WO}_3/\text{ZrO}_2\text{-Ce}_{0.6}\text{Zr}_{0.4}\text{O}_2$  (Co-prep) are also shown in Fig. 2. To identify the phases present in the mixed

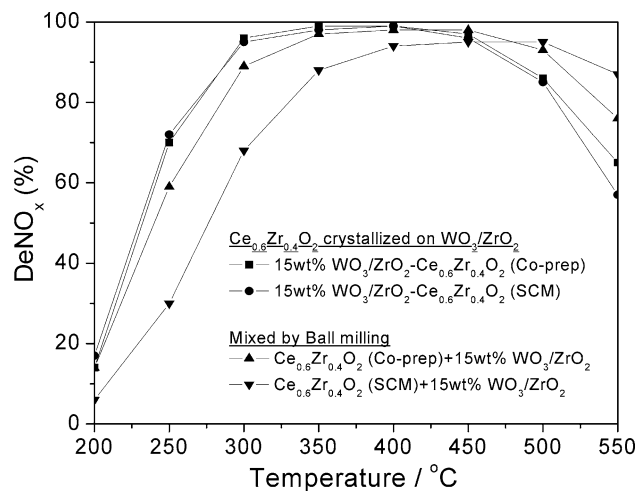


**Fig. 1**  $\text{NO}_x$  reduction efficiency over various 15 wt %  $\text{WO}_3/\text{ZrO}_2\text{-Ce}_{0.6}\text{Zr}_{0.4}\text{O}_2$  prepared by different way of mixing the components, i.e., 15 wt %  $\text{WO}_3/\text{ZrO}_2$  and  $\text{Ce}_{0.6}\text{Zr}_{0.4}\text{O}_2$ . Model gas: 1000 ppm  $\text{NO}$ , 1000 ppm  $\text{NH}_3$ , 10 %  $\text{O}_2$ , 5 %  $\text{H}_2\text{O}$  and  $\text{N}_2$  at GHSV = 50,000  $\text{h}^{-1}$

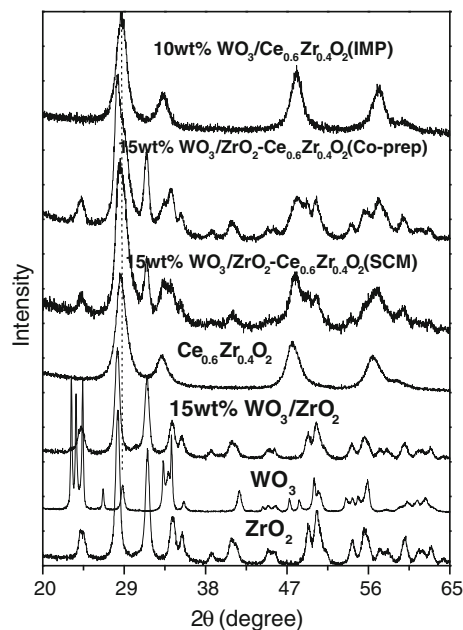


**Fig. 2** X-ray diffraction profile of  $\text{ZrO}_2$ ,  $\text{WO}_3$ , 15 wt %  $\text{WO}_3/\text{ZrO}_2$ ,  $\text{Ce}_{0.6}\text{Zr}_{0.4}\text{O}_2$ , 15 wt %  $\text{WO}_3/\text{ZrO}_2\text{-Ce}_{0.6}\text{Zr}_{0.4}\text{O}_2$  (SCM), 15 wt %  $\text{WO}_3/\text{ZrO}_2\text{-Ce}_{0.6}\text{Zr}_{0.4}\text{O}_2$  (Co-prep) and 10 wt %  $\text{WO}_3/\text{Ce}_{0.6}\text{Zr}_{0.4}\text{O}_2$  (IMP)

oxides, the characteristic reflections from pure  $\text{ZrO}_2$  and  $\text{WO}_3$  are also shown. Both  $\text{ZrO}_2$  and  $\text{WO}_3$  remained in the monoclinic structure after calcination at  $650^\circ\text{C}$ . Although, the presence of these oxides were expected in the mixed oxide catalyst there is no reflection at  $23^\circ$ , excluding the presence of  $\text{WO}_3$  crystallites in  $\text{WO}_3/\text{ZrO}_2$  and indicating finely dispersed  $\text{WO}_3$  on the  $\text{ZrO}_2$  surface.  $\text{Ce}_{0.6}\text{Zr}_{0.4}\text{O}_2$  on the  $\text{WO}_3/\text{ZrO}_2$  surface in the 15 wt %  $\text{WO}_3/\text{ZrO}_2\text{-Ce}_{0.6}\text{Zr}_{0.4}\text{O}_2$  (SCM) catalyst could not be detected because the peaks were overlapped with the  $\text{ZrO}_2$  peak. It is clearly visible that the peaks of 15 wt %  $\text{WO}_3/\text{ZrO}_2\text{-Ce}_{0.6}\text{Zr}_{0.4}\text{O}_2$  (SCM) are broader than of the 15 wt %  $\text{WO}_3/\text{ZrO}_2\text{-Ce}_{0.6}\text{Zr}_{0.4}\text{O}_2$  (Co-prep) catalyst indicating a smaller crystallite size in the SCM catalyst. The main peak in 15 wt %  $\text{WO}_3/\text{ZrO}_2\text{-Ce}_{0.6}\text{Zr}_{0.4}\text{O}_2$  (Co-prep) becomes unsymmetrical due to an overlap with the  $\text{ZrO}_2$  peak. Note that the relative intensity of the peaks remained the same confirming a homogeneous distribution of  $\text{Ce}_{0.6}\text{Zr}_{0.4}\text{O}_2$ . The formation of  $\text{Ce}_{0.6}\text{Zr}_{0.4}\text{O}_2$  was confirmed by the shift of the Raman band at around  $455\text{ cm}^{-1}$  with respect to  $\text{CeO}_2$ .

$\text{NH}_3$  TPD was used to determine the surface acidity which is required to bind ammonia at the surface as a condition for high  $\text{NO}_x$  reduction efficiencies. Figure 3 shows the  $\text{NH}_3$  desorption profiles over  $\text{Ce}_{0.6}\text{Zr}_{0.4}\text{O}_2$ , 15 wt %  $\text{WO}_3/\text{ZrO}_2$  and 15 wt %  $\text{WO}_3/\text{ZrO}_2\text{-Ce}_{0.6}\text{Zr}_{0.4}\text{O}_2$ . Pure  $\text{Ce}_{0.6}\text{Zr}_{0.4}\text{O}_2$  desorbs weakly adsorbed  $\text{NH}_3$  below  $350^\circ\text{C}$ . Since the  $\text{WO}_3/\text{ZrO}_2$  surface is strongly acidic, the  $\text{NH}_3$  desorption tail goes up to  $600^\circ\text{C}$  in 15 wt %  $\text{WO}_3/\text{ZrO}_2$ . A similar type of acidic sites is also present in 15 wt %  $\text{WO}_3/\text{ZrO}_2\text{-Ce}_{0.6}\text{Zr}_{0.4}\text{O}_2$  as evident from the desorption profile.

Figure 4a shows the  $\text{NO}_x$  reduction efficiency of the most promising catalyst 15 wt %  $\text{WO}_3/\text{ZrO}_2\text{-Ce}_{0.6}\text{Zr}_{0.4}\text{O}_2$  with varying space velocity from 20,000 to 50,000  $\text{h}^{-1}$ . Even at the highest space velocity of 50,000  $\text{h}^{-1}$  almost

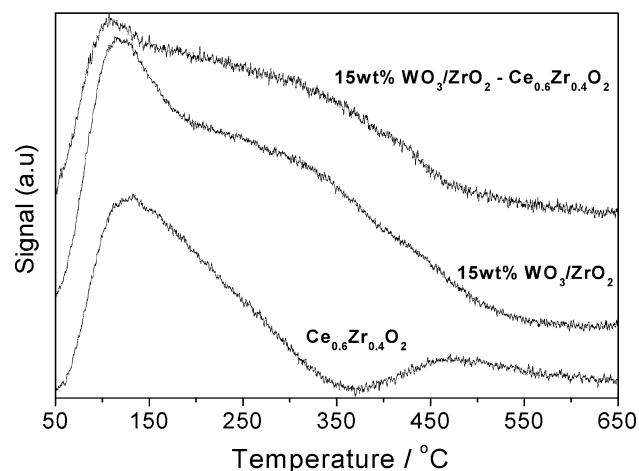


**Fig. 3**  $\text{NH}_3$ -TPD over  $\text{Ce}_{0.6}\text{Zr}_{0.4}\text{O}_2$ , 15 wt %  $\text{WO}_3/\text{ZrO}_2$  and 15 wt %  $\text{WO}_3/\text{ZrO}_2\text{-Ce}_{0.6}\text{Zr}_{0.4}\text{O}_2$

full conversion was measured between  $300$  to  $550^\circ\text{C}$ . Only below  $300^\circ\text{C}$ , a significant decrease in activity was observed with increasing space velocity. At low temperatures, the reaction rate became slow because the redox activity of  $\text{CeO}_2$  significantly decreased. Figure 4b shows the  $\text{NO}_x$  reduction efficiency ( $\text{DeNO}_x$ ) of this catalyst versus  $\text{NH}_3$  slip. This plot demonstrates that  $\text{DeNO}_x$  is high at 10 ppm  $\text{NH}_3$  emissions above  $300^\circ\text{C}$ . Moreover, the steeply rising curves confirm the high surface acidity of the catalyst, because already at rather low  $\text{NH}_3$  dosage the local  $\text{NH}_3$  concentration at the SCR sites are high enough to reach almost the maximum activity of the catalyst.

Figure 5 shows a comparison between the 15 wt %  $\text{WO}_3/\text{ZrO}_2\text{-Ce}_{0.6}\text{Zr}_{0.4}\text{O}_4$  catalyst and a commercial vanadium-based reference catalyst. It is obvious that there was no significant difference in  $\text{NO}_x$  reduction efficiency in the

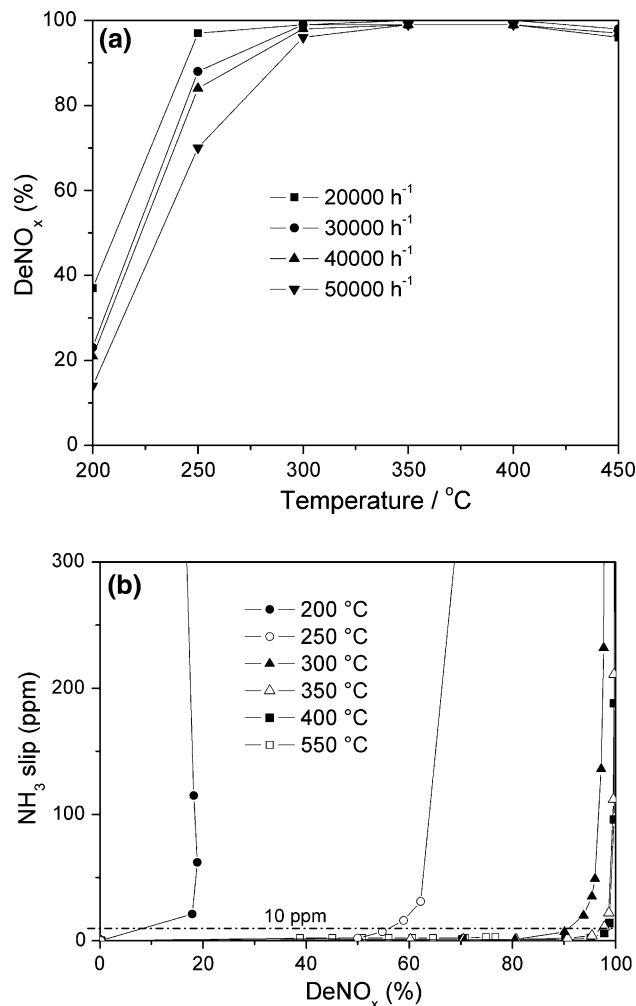


**Fig. 4** **a**  $\text{NO}_x$  reduction efficiency ( $\text{DeNO}_x$ ) vs temperature over 15 wt %  $\text{WO}_3/\text{ZrO}_2\text{-Ce}_{0.6}\text{Zr}_{0.4}\text{O}_2$  with varying space velocity. **b**  $\text{NH}_3$  slip vs  $\text{DeNO}_x$  over 15 wt %  $\text{WO}_3/\text{ZrO}_2\text{-Ce}_{0.6}\text{Zr}_{0.4}\text{O}_2$ . Model gas: 1000 ppm  $\text{NO}$ , 200–1500 ppm  $\text{NH}_3$ , 10 %  $\text{O}_2$ , 5 %  $\text{H}_2\text{O}$  and  $\text{N}_2$  as balance

temperature range from 250 to 550 °C. The reference catalyst produced much higher amounts of N<sub>2</sub>O above 450 °C compared to the 15 wt % WO<sub>3</sub>/ZrO<sub>2</sub>-Ce<sub>0.6</sub>Zr<sub>0.4</sub>O<sub>4</sub> catalyst, which on the other side produced slightly more N<sub>2</sub>O at lower temperatures. The 10 wt % WO<sub>3</sub>/Ce<sub>0.6</sub>Zr<sub>0.4</sub>O<sub>2</sub> catalyst, which was included in Fig. 5 for the purpose of comparison, showed a similar NO<sub>x</sub> reduction efficiency in the fresh state.

However, after hydrothermal aging substantial differences between these two catalysts became apparent, which are presented in Fig. 6. Hydrothermal ageing was performed successively at 675, 700 and 750 °C. The NO<sub>x</sub> reduction efficiency of the 15 wt % WO<sub>3</sub>/ZrO<sub>2</sub>-Ce<sub>0.6</sub>Zr<sub>0.4</sub>O<sub>2</sub> catalyst remained almost unchanged over the

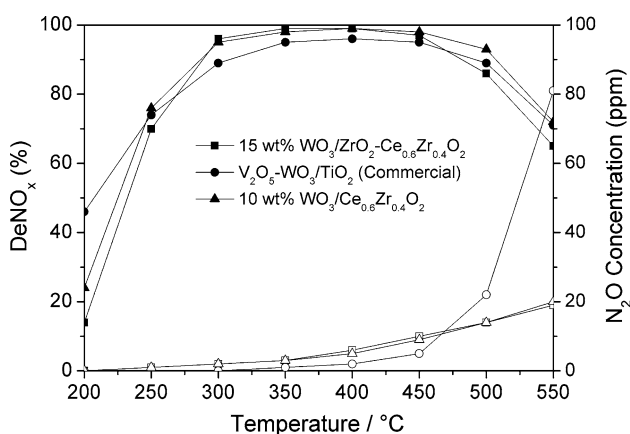


**Fig. 5** A comparison of NO<sub>x</sub> reduction efficiency between 15 wt % WO<sub>3</sub>/ZrO<sub>2</sub>-Ce<sub>0.6</sub>Zr<sub>0.4</sub>O<sub>2</sub> and reference catalysts V<sub>2</sub>O<sub>5</sub>-WO<sub>3</sub>/TiO<sub>2</sub> and 10wt % WO<sub>3</sub>/Ce<sub>0.6</sub>Zr<sub>0.4</sub>O<sub>2</sub>. Model gas: 1000 ppm NO, 1000 ppm NH<sub>3</sub>, 10 % O<sub>2</sub>, 5 % H<sub>2</sub>O and N<sub>2</sub> at GHSV = 50,000 h<sup>-1</sup>

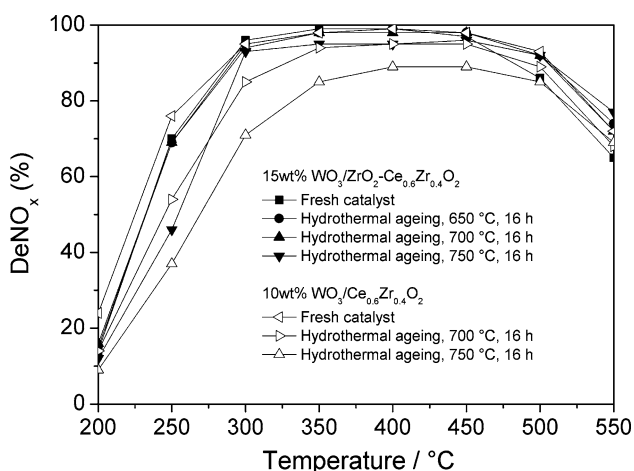


**Fig. 6** NO<sub>x</sub> reduction efficiency (closed symbols) and N<sub>2</sub>O emissions (open symbols) vs temperature of fresh and hydrothermally aged 15 wt % WO<sub>3</sub>/ZrO<sub>2</sub>-Ce<sub>0.6</sub>Zr<sub>0.4</sub>O<sub>2</sub> sample and 10 wt % WO<sub>3</sub>/Ce<sub>0.6</sub>Zr<sub>0.4</sub>O<sub>2</sub>. Model gas: 1000 ppm NO, 1000 ppm NH<sub>3</sub>, 10 % O<sub>2</sub>, 5 % H<sub>2</sub>O and N<sub>2</sub> at GHSV = 50,000 h<sup>-1</sup>

entire temperature range after hydrothermal treatment up to 700 °C. At 750 °C, there was some deactivation in activity mainly below 300 °C. Hydrothermal ageing of the 10 wt % WO<sub>3</sub>/Ce<sub>0.6</sub>Zr<sub>0.4</sub>O<sub>2</sub> catalyst started to decrease the NO<sub>x</sub> reduction efficiency significantly even at 700 °C and it went further down at 750 °C. The hydroxyl groups on the monoclinic ZrO<sub>2</sub> surface might be responsible for the observed differences by forming stronger bonds with WO<sub>3</sub> species than with the surface of Ce<sub>0.6</sub>Zr<sub>0.4</sub>O<sub>2</sub>. Since WO<sub>3</sub>/ZrO<sub>2</sub> is more stable than WO<sub>3</sub> alone, Ce<sub>0.6</sub>Zr<sub>0.4</sub>O<sub>2</sub> remains dispersed avoiding the loss of active sites.

The effect of SO<sub>2</sub> on the NO<sub>x</sub> reduction efficiency of the 10 wt % WO<sub>3</sub>/ZrO<sub>2</sub>-Ce<sub>0.6</sub>Zr<sub>0.4</sub>O<sub>2</sub> catalyst is presented in Fig. 7. After 5 h of SO<sub>2</sub> dosing, a promoting effect on the NO<sub>x</sub> reduction efficiency was observed at high temperatures, whereas the activity was decreased below 300 °C. At 550 °C, the NO<sub>x</sub> reduction efficiency increased from 65 to 76 %, while it decreased from 71 % to 46 % at 250 °C. The catalyst could be regenerated after heating in O<sub>2</sub> at 650 °C. The increase in activity at high temperatures could be due to an increase in acidity by the presence of sulfate groups. The presence of sulfate groups avoided ammonia oxidation leading to higher NO<sub>x</sub> reduction efficiencies at high temperature, while the surface coverage with sulfate reduced the redox property decreasing the NO<sub>x</sub> reduction efficiency at lower temperatures.

Figure 8 compares the SCR activity of 15 wt % WO<sub>3</sub>/ZrO<sub>2</sub>-Ce<sub>0.6</sub>Zr<sub>0.4</sub>O<sub>4</sub> with NH<sub>3</sub> gas and urea solution as reducing agents in the same reactor at 200, 250, 275 and 300 °C. The NH<sub>3</sub> slip-DeNO<sub>x</sub> curves show an identical behavior. The NO<sub>x</sub> reduction efficiency with urea solution was somewhat lower for some measurement points because Al<sub>2</sub>O<sub>3</sub> had to be added as catalyst binder in this experiment. This means that urea hydrolysis was also efficiently

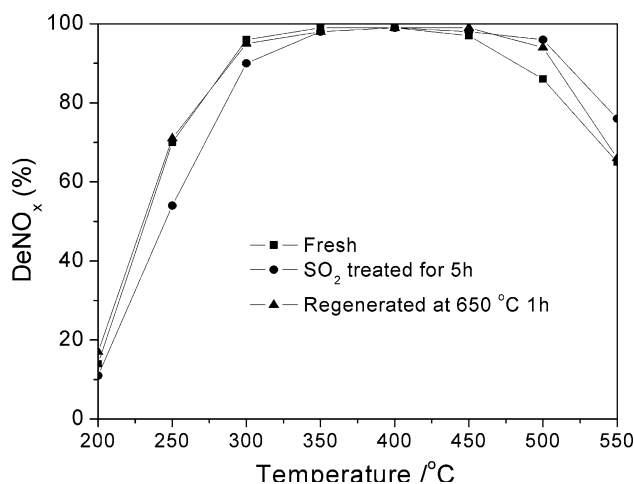


**Fig. 7** SCR activities of the fresh and 5 h SO<sub>2</sub>-poisoned and reactivated 15 wt % WO<sub>3</sub>/ZrO<sub>2</sub>-Ce<sub>0.6</sub>Zr<sub>0.4</sub>O<sub>2</sub>. Model gas: 1000 ppm NO, 1000 ppm NH<sub>3</sub>, 10 % O<sub>2</sub>, 5 % H<sub>2</sub>O and N<sub>2</sub> at GHSV = 50,000 h<sup>-1</sup>

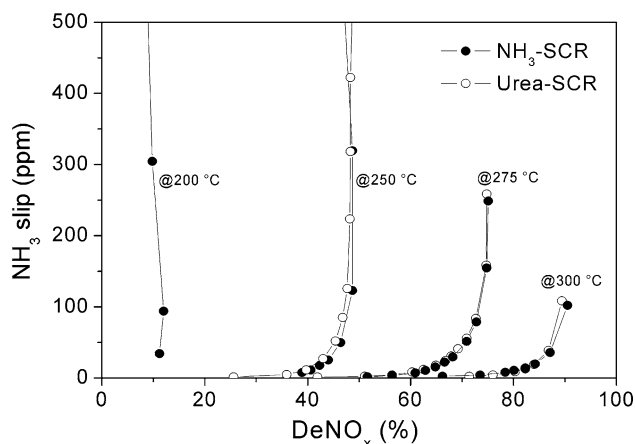


**Fig. 8**  $\text{NH}_3$  slip versus  $\text{DeNO}_x$  during urea and  $\text{NH}_3$  SCR over 15wt %  $\text{WO}_3/\text{ZrO}_2\text{-Ce}_{0.6}\text{Zr}_{0.4}\text{O}_2$ . Model gas: 1000 ppm  $\text{NO}$ , 1000 ppm  $\text{NH}_3$  (or the corresponding amount of urea), 10 %  $\text{O}_2$ , 5 %  $\text{H}_2\text{O}$  and  $\text{N}_2$  at  $\text{GHSV} = 50,000 \text{ h}^{-1}$

catalyzed, which renders the catalyst suitable for both stationary application with  $\text{NH}_3$  gas and mobile applications with urea solution.

#### 4 Conclusion

$\text{Ce}_{0.6}\text{Zr}_{0.4}\text{O}_2$  was grown on 15 wt %  $\text{WO}_3/\text{ZrO}_2$  yielding a highly stable 15 wt %  $\text{WO}_3/\text{ZrO}_2\text{-Ce}_{0.6}\text{Zr}_{0.4}\text{O}_2$  catalyst for the SCR process with  $\text{NH}_3$  and urea. The catalyst activity was completely unaffected by hydrothermal aging up to 700 °C. The  $\text{SO}_2$  treatment had only a limited effect on the SCR activity and the sample could be regenerated fully at 650 °C. The most important result regarding the application was that the  $\text{CeO}_2$  content in the catalyst could be reduced by 50 % by dispersing  $\text{Ce}_{0.6}\text{Zr}_{0.4}\text{O}_2$  on  $\text{WO}_3/\text{ZrO}_2$ , which kept the  $\text{NO}_x$  reduction efficiency at a similar level as the 10 wt %  $\text{WO}_3/\text{Ce}_{0.6}\text{Zr}_{0.4}\text{O}_2$  reference catalyst.

#### References

- Gabrielsson PLT (2004) *Top Catal* 28:177
- Koebel M, Elsener M, Kleemann M (2000) *Catal Today* 59:335
- Forzatti P (2001) *Appl Catal A* 222:221
- Centi G, Perathoner S (2007) *Stud Surf Sci Catal* 171:1
- Zheng HH, Keith JM (2004) *Catal Today* 98:403
- Trichard JM (2007) *Stud Surf Sci Catal* 171:211
- Madia G, Elsener M, Koebel M, Raimondi F, Wokaun A (2002) *Appl Catal B* 39:181
- Odenbrand CUI (2008) *Chem Eng Res Des* 86:663
- Kröcher O (2007) *Stud Surf Sci Catal* 171:261
- Kapteijn F, Singoredjo L, Andreini A, Moulijn JA (1994) *Appl. Catal. B* 3:173
- Singoredjo L, Korver R, Kapteijn F, Moulijn JA (1992) *Appl Catal B* 1:297
- Smirniotis PG, Pena DA, Uphade BS (2001) *Angew Chem Int Ed* 40:2479
- Wu Z, Jiang B, Liu Y, Zhao W, Guan B (2007) *J Hazard Mater* 145:488
- Qi G, Yang RT (2003) *J Catal* 217:434
- Qi G, Yang RT (2003) *Chem Commun* 2003:848
- Qi G, Yang RT (2003) *Appl Catal B* 44:217
- Qi G, Yang RT, Chang R (2003) *Catal Lett* 87:67
- Eigenmann F, Maciejewski M, Baiker A (2006) *Appl Catal B* 62:311
- Li Y, Cheng H, Li D, Qin Y, Xie Y, Wang S (2008) *Chem Commun* 2008:1470
- Casapu M, Kröcher O, Mehring M, Nachttegaal M, Borca C, Harfouche M, Grolimund D (2010) *J Phys Chem C* 114:9791
- Chen L, Li J, Ge M (2010) *Environ Sci Technol* 44:9590
- Casapu M, Bernhard A, Peitz D, Mehring M, Elsener M, Kröcher O (2011) *Appl Catal B* 103:79
- Shan W, Liu F, He H, Shi X, Zhang C (2011) *Chem Commun* 47:8046
- Verdier S, Rohard E, Bradshaw H, Harris D, Bichon Ph, Delahay G (2008) *SAE Technical Paper Series* 1:1022
- Putluru SSR, Riisagar A, Fehrmann R (2009) *Catal Lett* 133:370
- Patil KC, Aruna ST, Mimani T (2002) *Curr Opin Solid State Mater Sci* 6:507